Results in Engineering 26 (2025) 105587

Contents lists available at ScienceDirect

Results in Engineering

journal homepage: www.sciencedirect.com/journal/results-in-engineering

Research paper

# Development and characterization of an epoxy matrix composite reinforced with $Al_2O_3$ embedded banyan fibers for secondary structural applications

Baskar S [a], Ganesan Subbiah [b], Padma Priya G [c], Guntaj J [d], Mukesh Kumar [e], Kamakshi Priya K [f], Nandagopal Kaliappan [g,h,*]

[a] Department of Automobile Engineering, Vels Institute of Science, Technology & Advanced Studies, Chennai - 600 117, Tamil Nadu, India
[b] Department of Mechanical Engineering, Sathyabama (Deemed to be University), Chennai, Karnataka, India
[c] Department of Mechanical Engineering, Jain (Deemed to be University), Bangalore, Karnataka, India
[d] Centre for Research Impact and Outcome, Chitkara Institute of Engineering and Technology, Chitkara University, Rajpura, Punjab, India
[e] Deaprtment of Mechanical Engineering, Vivekananda Global University, Jaipur, India
[f] Department of Physics, Saveetha School of Engineering, SIMATS, Saveetha University, Chennai, Tamil Nadu, India
[g] Department of Mechanical Engineering, Haramaya Institute of Technology, Haramaya University, Dire Dawa, Ethiopia
[h] Department of Food Technology, Dhanalakshmi Srinivasan College of Engineering, Coimbatore, Tamil Nadu, India

ARTICLE INFO

*Keywords:*
Nanoparticles
Sustainable development
Natural fiber
Ceramic particles
Structural analysis
Surface morphology

ABSTRACT

The demand for sustainable, high-performance composites is increasing in industries such as automotive, aerospace, and construction. However, conventional fiber-reinforced polymer composites suffer from environmental limitations, poor bioactivity, and fatigue susceptibility. This study develops a novel epoxy matrix composite reinforced with 3 % (12 g) $Al_2O_3$ embedded banyan fibers to enhance mechanical strength and bioactivity. Experimental analysis demonstrates notable improvements in the sample with 12 g $Al_2O_3$, tensile strength (67.49 MPa), flexural strength (69.38 MPa), impact energy (19.47 kJ/m$^2$), and Shore D hardness (47). Fatigue testing confirms durability, withstanding 40 MPa stress for 14,000 cycles due to improved fiber-matrix bonding and uniform filler dispersion. Scanning Electron Microscopy validates structural integrity, while antibacterial assessments show a 12 mm inhibition zone against Streptococcus pyogenes and significant biofilm reduction via Confocal Laser Scanning Microscopy. These findings highlight the composite's potential for applications requiring mechanical durability and bioactivity, including medical devices and bioactive environments.

## 1. Introduction

The growing demand for advanced composite materials with enhanced mechanical, thermal, and chemical properties has driven extensive research into sustainable and cost-effective alternatives [1]. Industries such as automotive, aerospace, and construction increasingly seek materials that combine high performance with eco-friendliness to meet stringent environmental regulations and reduce carbon footprints [2]. In this context, natural fiber-reinforced polymer composites have garnered significant attention due to their lightweight nature, renewability, biodegradability, and superior mechanical properties [3]. These materials align with the global push toward sustainable manufacturing practices while addressing performance demands. Among the diverse range of natural fibers, banyan fibers remain largely underutilized, despite their widespread availability, low cost, and excellent tensile properties [4]. These fibers offer significant potential for material innovation due to their inherent strength and compatibility with various polymer matrices. However, limited research has explored their application in advanced composites, leaving a gap in understanding their full potential [5]. Integrating banyan fibers into polymer composites could lead to the development of materials with competitive performance and reduced reliance on synthetic fibers [6]. Composite materials, particularly those using epoxy as a matrix, are widely recognized for their superior strength-to-weight ratio, corrosion resistance, and durability, making them indispensable in high-performance applications across industries such as aerospace, automotive, and marine [7]. The increasing push for sustainability in material science has highlighted the integration of natural fibers into these composites as an eco-friendly alternative to synthetic fibers, addressing the environmental concerns associated with the production and disposal of traditional materials like

* Corresponding author.
*E-mail address:* nandagopal.kaliappan@haramaya.edu.et (N. Kaliappan).

https://doi.org/10.1016/j.rineng.2025.105587
Received 30 November 2024; Received in revised form 29 May 2025; Accepted 1 June 2025
Available online 1 June 2025

glass and carbon fibers [8]. Natural fibers such as jute, flax, hemp, and sisal have gained significant attention due to their renewability, biodegradability, and ability to significantly reduce the carbon footprint of composite materials [9]. As of 2023, global production of natural fibers reached 30 million tons, reflecting their abundant availability and diverse applicability [10]. Moreover, the utilization of natural fibers in composite applications has exhibited a 10 % annual growth rate over the past five years, driven by advancements in material processing and growing awareness of their environmental benefits [11]. Despite this growth, natural fiber-reinforced composites face challenges, particularly their relatively lower mechanical properties, moisture sensitivity, and variability in fiber quality compared to synthetic counterparts [12]. To address these limitations, researchers have focused on the incorporation of nano-scale fillers such as aluminum oxide ($Al_2O_3$). $Al_2O_3$ is renowned for its exceptional hardness, thermal stability, and wear resistance, properties that significantly enhance the performance of polymer composites. Its addition to natural fiber-reinforced epoxy composites not only improves mechanical strength and thermal stability but also enhances interfacial bonding between the matrix and fibers, overcoming the inherent weaknesses of natural fibers [13]. This synergistic effect results in composites with improved load-bearing capacity, reduced water absorption, and enhanced durability under varying environmental conditions. Furthermore, the development of hybrid composites using $Al_2O_3$-embedded natural fibers provides a promising pathway for tailoring material properties to specific applications. By carefully optimizing the fiber-matrix-filler interactions, these composites can achieve performance levels comparable to or even surpassing those of conventional synthetic composites [14]. Banyan fibers, extracted from the aerial roots of the *Ficus benghalensis* tree, present a unique and largely underutilized potential in composite material development. With tensile strengths ranging from 18 to 25 MPa, these fibers compare favorably with other widely used natural fibers such as jute and hemp, making them viable candidates for reinforcement applications in high-performance composites. Despite their promising mechanical properties and abundant availability, banyan fibers remain significantly underexplored in material science, representing a missed opportunity in the search for sustainable and cost-effective alternatives to synthetic reinforcements [15]. The chemical composition of banyan fibers plays a crucial role in their mechanical performance. Their cellulose content, estimated at 55–60 %, ensures high stiffness and tensile strength, while the relatively low lignin percentage (15–20 %) minimizes brittleness and enhances flexibility. This combination of properties facilitates efficient load transfer within polymer matrices, a critical requirement for composite applications [16]. The fibers' low hemicellulose content further contributes to their stability, reducing water absorption and improving durability under humid conditions. An additional advantage of banyan fibers lies in their hierarchical structure, characterized by a natural microfibrillar arrangement that provides a high surface area and a porous network. This structure enhances their ability to undergo chemical modifications, such as alkali treatment, salinization, and grafting with functional groups [17]. Banyan fibers offer distinct advantages, including higher biodegradability, making them more environmentally sustainable than some other fibers. Additionally, they exhibit inherent antimicrobial properties, which are particularly beneficial for hygiene-related applications like toothbrush bristles. Furthermore, banyan fibers are cost-effective and widely available as a by-product in certain regions, providing an affordable alternative to conventional fibers. These unique attributes strengthen the case for their use as a sustainable and functional material [18]. Being a renewable resource with minimal cultivation requirements, they are a low-cost alternative to synthetic fibers, which involve energy-intensive manufacturing processes. Their use in composites aligns with global sustainability goals, offering a pathway to reduce dependence on non-renewable resources while minimizing waste [19]. The potential applications of banyan fiber-reinforced composites extend across various industries. In the automotive sector, they can be used for lightweight interior panels, underbody shields, and seat structures, contributing to fuel efficiency and reduced emissions [20]. In construction, their high tensile strength and durability make them suitable for secondary structural components, such as roofing and wall cladding. Additionally, their bio-based origin and superior mechanical properties offer a viable solution for the aerospace industry's demand for lightweight, high-strength materials. Aluminum oxide nanoparticles have shown promise in enhancing the mechanical and thermal properties of polymer composites [21]. Their exceptional hardness (15–20 GPa) and high thermal conductivity (30–35 W/mK) provide an ideal filler for load-bearing and heat-dissipating applications. Additionally, the high surface area of $Al_2O_3$ nanoparticles ensures improved adhesion with the matrix, leading to a uniform stress distribution. Studies have shown that incorporating 2–5 wt. % $Al_2O_3$ nanoparticles into epoxy-based composites can improve tensile strength by up to 25 % and 30 % of flexural strength. This approach bridges the gap between sustainability and performance, enabling the broader adoption of natural fiber composites in demanding structural applications [22]. The economic and environmental implications of this research are significant. By leveraging abundant, low-cost natural fibers and incorporating high-performance fillers like $Al_2O_3$, manufacturers can produce cost-effective, lightweight, and environmentally friendly materials suitable for a wide range of applications. Such advancements contribute to the circular economy by promoting resource efficiency, reducing waste, and minimizing environmental impact. As industries increasingly prioritize sustainability, the adoption of advanced natural fiber-reinforced composites represents a transformative step toward greener, more resilient material solutions [23]. By developing a durable, bioactive, and eco-friendly composite, this study supports advancements in sustainable manufacturing, promotes the use of natural fibers to reduce environmental impact, and enhances materials for biomedical applications. These aspects align with global efforts to improve infrastructure, resource efficiency, and human well-being, reinforcing the broader significance of our research.

This study investigates the development and characterization of a novel epoxy matrix composite reinforced with aluminium oxide ($Al_2O_3$) filler embedded banyan fibers to address the limitations of conventional fiber-reinforced polymer composites, such as inadequate mechanical strength, fatigue resistance, and bioactivity. In the present study, bioactivity is specifically defined as the antibacterial performance of the composite materials, characterized by their ability to inhibit or reduce bacterial growth. This usage is distinct from the traditional materials science context, where bioactivity refers to osteoconductivity, biocompatibility, or the promotion of tissue integration. The findings demonstrate significant improvements in mechanical properties, fatigue performance, and antibacterial efficacy, positioning this composite as a promising material for applications demanding superior strength, longevity, and bioactivity.

## 2. Materials and experimental methods

Araldite Ly556 epoxy resin serves as the primary matrix material, cured with HY951 hardener in a precise 10:1 wt ratio to ensure significant cross-linking and mechanical strength. Additionally, chopped banyan fibers, measuring 10 to 15 cm in length, are used as a natural reinforcement, contributing to the composite's sustainability, lightweight structure, and mechanical performance. The raw materials, including the banyan fibers and fillers, are sourced from Go Green Composites, Chennai, India, a trusted supplier known for quality and consistency. The general properties of banyan fiber, aluminium oxide nanoparticles, epoxy resin and hardener were given in Tables 1–4.

### 2.1. Fabrication process of banyan fiber composite

The hand layup method was employed for fabricating banyan fiber-reinforced $Al_2O_3$ particle-blended epoxy matrix composites due to its

**Table 1**
Properties of banyan fiber [courtesy: Go Green Composites].

| Properties | Banyan Fiber |
|---|---|
| Category | Natural Fiber |
| Type | Chopped Fiber |
| Fibre diameter | 200 μm (avg) |
| Density | 1.97 g/cc |

**Table 2**
Properties of aluminium oxide nanoparticles [courtesy: Go Green Composites].

| Properties | Value |
|---|---|
| Density (g/cm$^3$) | 3.95 |
| Particle Size (nm) | −190.0 |
| Surface Area (m$^2$/g) | −110.0 |
| Melting Point ( °C) | 2072.0 |
| Boiling Point ( °C) | 2977.0 |
| Hardness (Mohs) | 9.0 |
| Young's Modulus (GPa) | 38.0 |
| Thermal Conductivity (W/mK) | 30.0 |

**Table 3**
Properties of bisphenol-F LY556 epoxy polymer [courtesy: Go Green Composites].

| Aspect (visual) | Clear liquid |
|---|---|
| Density at 25 °C | 1.2 g/cc |
| Viscosity at 25 °C | 10–12 Pa.s |
| Curing Temperature | 80 °C |
| Glass Transition Temperature | 140 °C |

**Table 4**
Properties of Araldite HY 951 Hardener [courtesy: Go Green Composites].

| Flash Point | 110 °C |
|---|---|
| Mix Ratio | 100:10 |
| Specific Gravity | 0.98 g/cm$^3$ at 25 °C |

simplicity and cost-effectiveness. The process began with the preparation of raw materials, including banyan fibers, $Al_2O_3$ particles, and epoxy resin (Hy951 with LY 556 hardener in a 10:1 ratio). To enhance fiber-matrix adhesion, banyan fibers underwent alkali treatment (5 % NaOH for 4 h), which removed surface impurities and exposed cellulose microfibrils, improving mechanical interlocking [24]. The treated fibers were then mixed with epoxy resin and $Al_2O_3$ particles using a mechanical stirrer at 500 rpm for 30 min to ensure homogeneity. Before fabrication, a polymer-based releasing agent was applied to the mold to facilitate easy demoulding. The composite was fabricated by sequentially layering epoxy-$Al_2O_3$ mixture and randomly oriented banyan fibers, ensuring uniform fiber distribution and thorough impregnation using rollers to eliminate air bubbles. A weighted plate was applied to improve consolidation and minimize voids, followed by curing at room temperature for 48 h and post-curing at 95 °C for 2 h to enhance mechanical stability. A 1 %–5 % $Al_2O_3$ particle range was selected based on preliminary trials, as lower concentrations (<1 %) provided inadequate reinforcement, while higher concentrations (>5 %) led to filler agglomeration and poor fiber-matrix bonding. The weight ratio of materials used to fabricate the composite was given in the Table 5.

### 2.2. Testing process of banyan fiber composite

The testing process for banyan fiber-reinforced $Al_2O_3$ particle epoxy composites involve comprehensive evaluations to determine their mechanical, thermal, and antibacterial properties, adhering to ASTM standards. Fig. 1 shows the tested samples of banyan fiber composite.

**Table 5**
The weight ratio of materials used to fabricate the composite.

| Sample code | Banyan fiber in g | Al2O3 filler in g | Epoxy matrix in g |
|---|---|---|---|
| B1 | 200 | 4 (1 %) | 198 |
| B2 | 200 | 8 (2 %) | 196 |
| B3 | 200 | 12 (3 %) | 194 |
| B4 | 200 | 16 (4 %) | 192 |
| B5 | 200 | 20 (5 %) | 190 |

#### 2.2.1. Tensile test

Tensile strength testing was performed using a Universal Testing Machine (INSTRON 5967) in accordance with ASTM D3039 standards. The specimens were carefully prepared with dimensions of 250 mm × 25 mm × 3 mm to ensure uniformity and reliability in testing. During the experiment, a uniaxial tensile load was applied at a crosshead speed of 2 mm/min, simulating real-world stress conditions. The tests were conducted under controlled ambient conditions (23 ± 2 °C, 50 % RH) to minimize environmental influences on the material's performance. Data from the tests were recorded in terms of ultimate tensile strength, strain-to-failure, and Young's modulus, providing insights into the composite's mechanical integrity and reinforcement efficiency.

#### 2.2.2. Flexural test

The flexural strength of the banyan fiber-reinforced $Al_2O_3$ particle epoxy composites was determined using a three-point bending test in accordance with ASTM D790. Rectangular test specimens, measuring 127 mm × 12.7 mm × 3 mm, were subjected to bending forces with a span-to-thickness ratio of 16:1 to ensure precise stress distribution and accurate evaluation of flexural properties. This testing method provides essential insights into the stiffness, load-bearing capacity, and deformation resistance of the composite, highlighting its structural performance under bending loads.

#### 2.2.3. Izod impact test

The impact resistance of the banyan fiber-reinforced $Al_2O_3$ particle epoxy composites were evaluated using a Tinius Olsen IT406 Izod Impact Tester, following the ASTM D256 standard. Notched specimens with dimensions 63.5 mm × 12.7 mm × 3 mm were tested at room temperature to determine the composite's ability to withstand sudden impact loads. The test involved striking the specimen with a pendulum hammer to measure the energy absorbed during fracture, providing insights into the composite's toughness, notch sensitivity, and fracture resistance.

#### 2.2.4. Shore D hardness test

The surface hardness of the banyan fiber-reinforced $Al_2O_3$ particle epoxy composites was evaluated using a Shore D hardness test, following the ASTM D2240 standard. Test specimens measuring 50 mm × 50 mm × 3 mm were prepared and conditioned to ensure uniformity and accuracy. The Shore D durometer was applied with a constant force, and the hardness values were recorded after a dwell time of 15 s to assess the material's resistance to surface deformation. This method is particularly suitable for polymer-based composites, providing a reliable measure of indentation hardness, scratch resistance, and wear durability [25].

#### 2.2.5. Fatigue test

The fatigue behavior of the banyan fiber-reinforced $Al_2O_3$ particle epoxy composites was investigated using a Servo-hydraulic Fatigue Testing Machine (MTS Landmark 370.10), following the ASTM E466 standard. Cyclic loading was applied to precisely machined test specimens with dimensions 150 mm × 10 mm × 3 mm, ensuring uniform

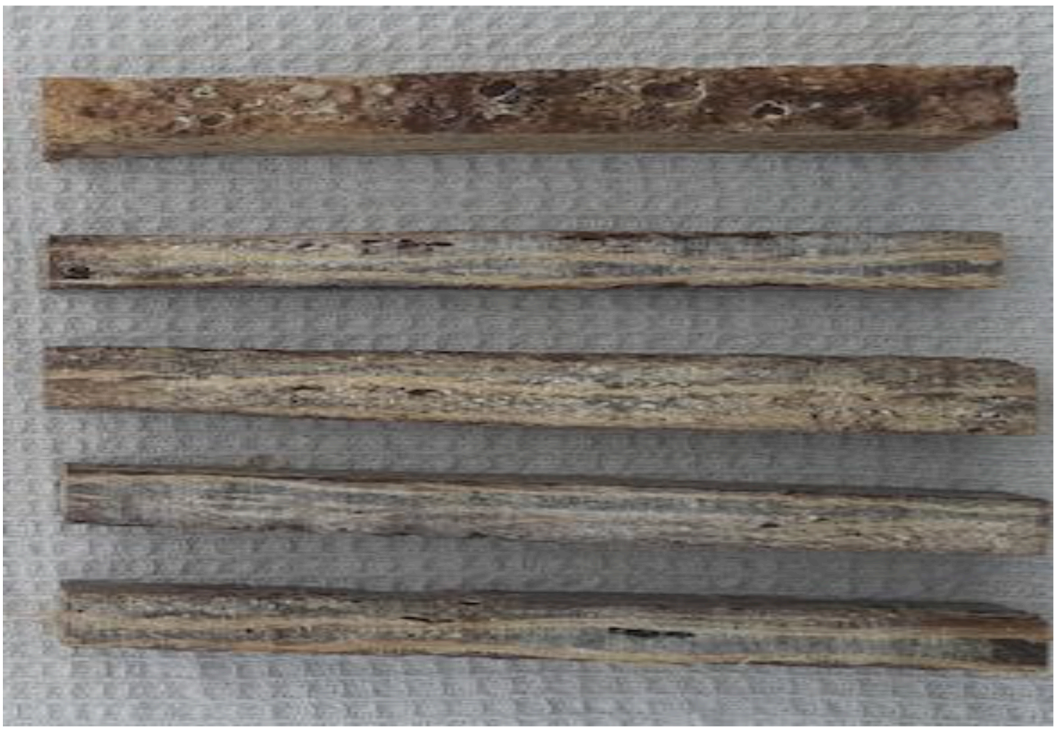

**Fig. 1.** Tested samples of banyan fiber composite.

stress distribution. The tests were conducted at a loading frequency of 5 Hz with a stress ratio (R) of 0.1, representing tension-tension fatigue loading conditions. This experimental setup allowed for the evaluation of the composite's fatigue life, damage accumulation, and resistance to progressive failure under repeated stress cycles.

#### 2.2.6. SEM test

The microstructural analysis of the banyan fiber-reinforced $Al_2O_3$ particle epoxy composites was conducted using a Field Emission Scanning Electron Microscope (FE-SEM, ZEISS Gemini SEM 500), operated at an accelerating voltage of 5–15 kV. Prior to imaging, the samples were sputter-coated with a thin layer of gold to enhance conductivity and improve image resolution. This analysis provided detailed insights into the fiber-matrix interactions, dispersion of $Al_2O_3$ particles, interfacial bonding quality, and failure mechanisms at the microstructural level. High-resolution micrographs were obtained to examine void formation, fiber pull-out, matrix cracking, and agglomeration of reinforcement particles, which play a critical role in determining the composite's mechanical strength, durability, and failure behavior. Simultaneous EDX analysis is conducted to determine the elemental composition, confirming the presence of oxygen, carbon, and other characteristic elements associated with composite material. The study also focused on fracture surface morphology, assessing the degree of adhesion between fibers and the epoxy matrix, as well as the uniformity of particle distribution [26].

#### 2.2.7. Antibacterial test

The antibacterial activity of the banyan fiber-reinforced $Al_2O_3$ particle epoxy composites against *Streptococcus pyogenes* was assessed using the agar well diffusion method. Sterile composite discs (10 mm × 2 mm) were placed on bacteria-inoculated agar plates and incubated at 37 °C for 24 h. The zones of inhibition (ZOI) were measured in millimeters to evaluate bacterial growth suppression. The antibacterial effect was attributed to the $Al_2O_3$ nanoparticles, known for their antimicrobial properties. Varying the concentrations of composite samples was compared to standard antibacterial agent *Streptomycin* used for validation, and the findings suggest potential applications in biomedical, dental, and antibacterial surface coatings, combining mechanical strength with antimicrobial resistance.

#### 2.2.8. Biofilm analysis

Confocal microscopy analysis was performed using a Leica TCS SP8 Confocal Laser Scanning Microscope to examine bacterial adhesion and biofilm formation on the surface of the banyan fiber-reinforced $Al_2O_3$ particle epoxy composites. To enhance visualization, bacterial cells were stained with fluorescent dyes, such as SYTO 9 for live cells and propidium iodide (PI) for dead cells, enabling a clear distinction between viable and non-viable bacteria. Imaging was carried out at 40 × magnification under specific excitation wavelengths (488 nm for SYTO 9 and 561 nm for PI) to capture high-resolution images of bacterial colonization. Additionally, image analysis software was used to quantify biovolume, surface coverage, and bacterial viability, providing a comprehensive understanding of biofilm formation dynamics. The study aimed to correlate bacterial adhesion with the surface roughness, hydrophobicity, and chemical composition of the composite, helping to evaluate its potential for antimicrobial applications [27]. These tests ensure a thorough characterization of mechanical, morphological, and antibacterial properties, confirming the composite's suitability for industrial and biomedical applications.

## 3. Results and discussion

Comprehensive analysis of the observed mechanical properties, exploring the influence of fiber reinforcement, $Al_2O_3$ particle dispersion, and interfacial bonding on tensile, flexural, impact, and hardness characteristics.

### 3.1. Tensile strength

Fig. 2 shows the tensile strength of banyan fiber composite. Five different samples, labeled B1 to B5, were tested, with each incorporating varying concentrations of $Al_2O_3$ particle fillers. Among these, Sample B3, which contained 3 % (12 g) $Al_2O_3$ filler, exhibited the highest tensile strength of 67.49 MPa, indicating improved reinforcement due to the

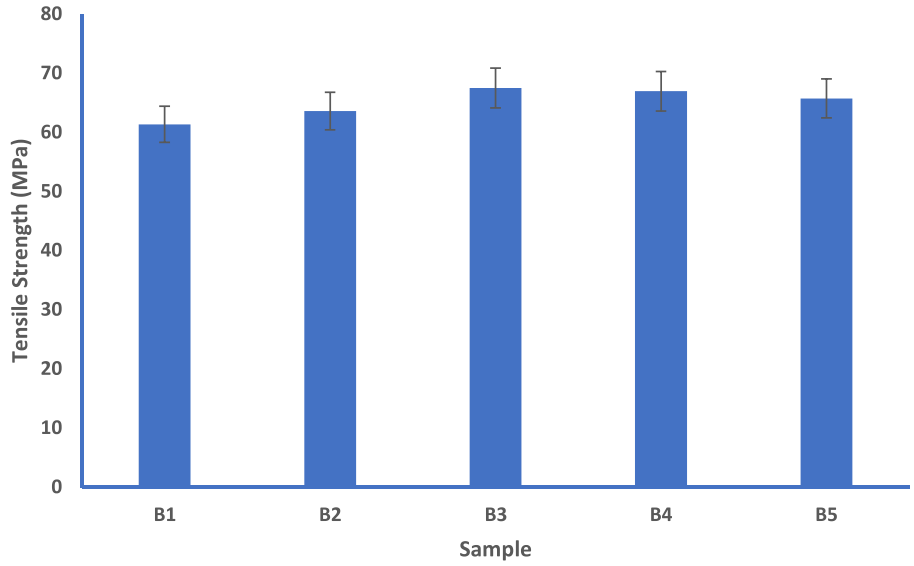


**Fig. 2.** Tensile strength of banyan fiber composite.

effective dispersion of particles and enhanced fiber-matrix interaction. This superior strength can be attributed to the balance between the filler content and the matrix, resulting in improved load transfer efficiency. Studies indicate that incorporating 10–20 % jute fibers and 5–10 % aluminium oxide particles into the epoxy matrix can enhance the tensile strength values ranging between 55 MPa and 65 MPa. The study was found on the pure epoxy matrix composites generally exhibit moderate mechanical properties due to their brittle nature. The tensile strength of 20.3 MPa, reflecting limited load-bearing capacity [28]. In another study, the banyan fiber-reinforced epoxy matrix composites exhibit significant improvements in mechanical properties compared to the pure epoxy matrix. Literature reports that the tensile strength of such composites 30.92 MPa. The alkali treatment of fibers enhances fiber-matrix bonding, leading to better stress transfer and increased strength [29]. This combination achieves a balance of lightweight and high-strength properties, making it suitable for structural applications. In comparison, Sample B1, with the lowest filler concentration, showed the minimum tensile strength of 61.34 MPa, which reflects weaker interfacial bonding and lower reinforcement effectiveness. Sample B2, containing 2 % (8 g) $Al_2O_3$ filler, exhibited a moderate tensile strength of 63.57 MPa, suggesting a partial improvement in mechanical properties due to increased filler-matrix interactions. Similarly, Sample B4 and Sample B5, with filler concentrations of 4 % (16 g) and 5 % (20 g), demonstrated tensile strengths of 66.93 MPa and 65.72 MPa, respectively. While these values are significantly higher than those of B1 and B2, they did not surpass B3, likely due to the agglomeration of particles at higher filler concentrations, which can create stress concentration points and reduce the composite's ability to bear loads effectively. Fig. 3 shows the stress vs strain curve of banyan fiber composite.

The stress-strain curves indicate that the 3 % $Al_2O_3$ filler

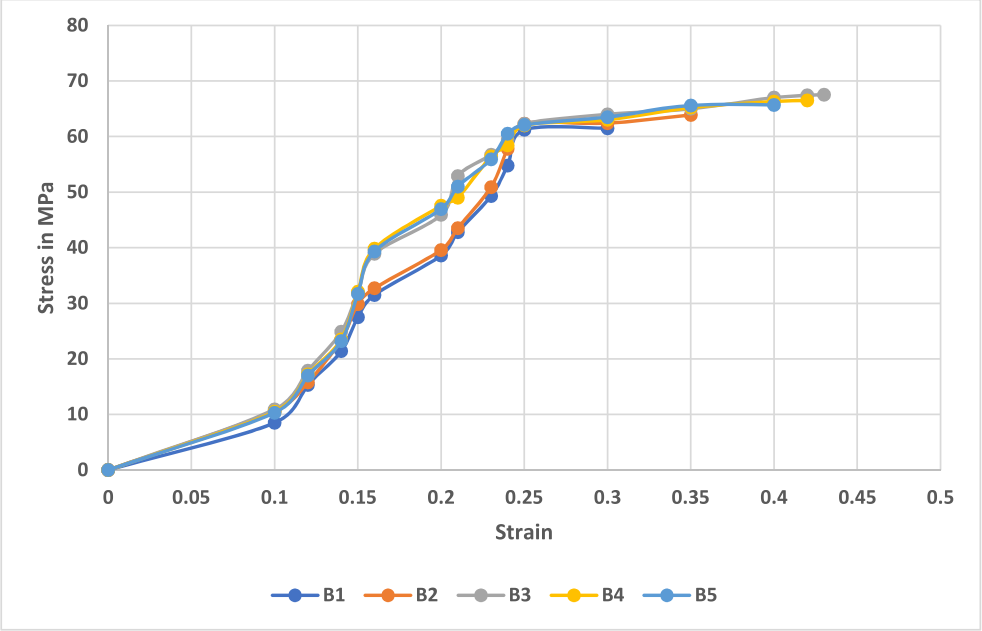


**Fig. 3.** The stress vs strain curve of banyan fiber composite.

concentration (B3) exhibits the highest tensile strength and an optimal balance between stress and strain. This performance is attributed to uniform filler dispersion, which enhances fiber-matrix bonding and stress transfer efficiency. For lower filler concentrations (B1 and B2), the stress-strain curves show reduced tensile strength, likely due to insufficient reinforcement, where the $Al_2O_3$ particles are not present in sufficient quantities to significantly improve mechanical properties. In contrast, higher filler concentrations (B4 and B5) exhibit diminished tensile strength and strain capacity, primarily due to particle agglomeration, which creates stress concentration points, reduces effective load transfer, and leads to premature failure. The Young's modulus was determined from the initial linear region of the stress–strain graph, showing that Sample B1 exhibited 3.80 MPa, B2 around 3.9 MPa, B3 reached the highest at 4.15 MPa, followed by B4 at 4.05 MPa and B5 at 3.95 MPa. This indicates that Sample B3, corresponding to the 15 g porcelain filler loading, achieved the highest stiffness among the tested composites. The strain at failure, representing the material's ductility, was extracted as 0.41 for B1, 0.42 for B2, 0.43 for B3, 0.42 for B4, and 0.41 for B5, again highlighting that Sample B3 maintained superior ductility. These comprehensive findings demonstrate that the optimal porcelain filler loading in Sample B3 not only improved the tensile strength and stiffness but also enhanced the toughness and maintained favourable ductility, thus providing a balanced enhancement of mechanical performance.

### 3.2. Flexural strength

Fig. 4 shows the flexural strength of banyan fiber composite. The superior flexural strength of B3 reflects its enhanced load transfer efficiency and resistance to deformation under bending stress. In contrast, Sample B1, with minimal filler content, showed the lowest flexural strength of 64.81 MPa, highlighting the insufficient reinforcement of the matrix and weaker fiber-matrix interactions. In another research, banyan fiber/epoxy matrix composite reveals the flexural strength falls with 34.28 MPa [30]. Sample B2, with a 2 % (8 g) $Al_2O_3$ filler concentration, demonstrated a slight improvement, achieving a flexural strength of 65.47 MPa, indicating some reinforcement but still not enough for maximizing strength. Similarly, Sample B4 and Sample B5, containing 4 % (16 g) and 5 % (20 g) $Al_2O_3$ fillers, exhibited flexural strengths of 68.51 MPa and 67.49 MPa, respectively. These values are close to the maximum strength achieved by B3 but slightly lower, likely due to particle agglomeration at higher filler concentrations, which can create stress concentration points and negatively impact the composite's ability to resist bending forces. The observed trend suggests that a 3 % (12 g) $Al_2O_3$ filler concentration provides a good balance between filler dispersion, matrix integrity, and fiber reinforcement. At this concentration, the $Al_2O_3$ particles effectively enhance the matrix stiffness without introducing significant defects or aggregation. In another research, sisal fiber-reinforced sawdust particle epoxy matrix composites demonstrate significant flexural strength enhancements due to the combined reinforcement of natural fibers and lignocellulosic particles. Experimental studies reveal that composites with 15–25 % sisal fibers and 5–10 % sawdust particles achieve flexural strength values in the range of 50–60 MPa, compared to 40 MPa for the neat epoxy matrix [31]. In comparison, banyan fiber-reinforced $Al_2O_3$ particles epoxy composites exhibit slightly higher flexural strength, with values ranging from 64 to 69 MPa under similar reinforcement conditions. This difference can be attributed to the superior bonding capability and higher mechanical properties of banyan fibers with $Al_2O_3$ particles, which contribute to better stress transfer and flexural resistance. The higher flexural strength of Sample B3 makes it a potential material for applications requiring materials with high bending resistance, such as in automotive interior panels, structural components, and lightweight construction materials. Fig. 5 shows the flexural stress vs strain curve of banyan fiber composite.

The stress vs. strain curve from the flexural test of banyan fiber-reinforced aluminium oxide particulate epoxy matrix composites reveals a nNar relationship, indicating progressive loading and failure behavior. Samples B1, B2, B3, B4, and B5 exhibit maximum flexural stress values in the range of 64–69 MPa, with B3 showing the highest flexural stress of approximately 69.38 MPa before failure. The strain values at peak stress range between 0.4 and 0.5, highlighting the composite's ductile nature. Flexural strain at failure was determined from the stress–strain curves by identifying the strain corresponding to the maximum stress prior to material fracture. The extracted flexural strain at failure values were approximately 0.50 for Sample B1, 0.52 for B2, 0.55 for B3, 0.52 for B4, and 0.51 for B5. Among all samples, Sample B3 demonstrated the highest flexural strain at failure (~0.55), signifying

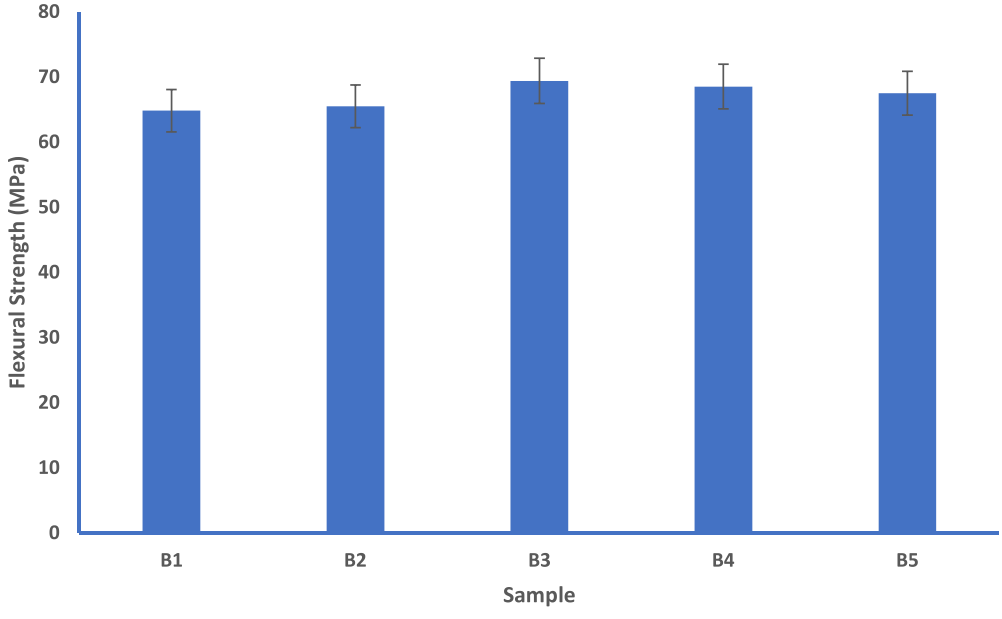


**Fig. 4.** Flexural strength of banyan fiber composite.

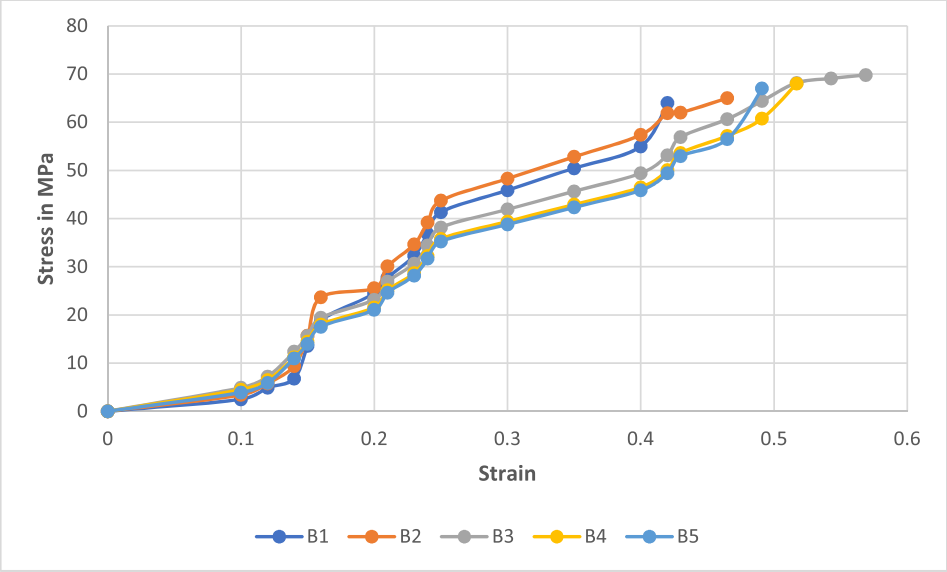


**Fig. 5.** Flexural stress vs strain curve of banyan fiber composite.

enhanced flexibility, greater deformation capability, and superior energy absorption potential under flexural loading conditions. The higher flexural strain at failure observed in B3 suggests that the optimized porcelain filler content (15 g) facilitated an improved stress distribution within the epoxy matrix, delaying the onset of microcracking and allowing the composite to endure greater strain before catastrophic failure. This behavior is indicative of a tougher and more resilient composite structure, capable of sustaining larger deformations without losing structural integrity. The improved flexibility of B3 can be attributed to the homogenous dispersion of fillers and the effective stress transfer across the matrix–fiber interface, minimizing local stress concentrations. In contrast, the comparatively lower flexural strain at failure in B1, B2, B4, and B5 implies that either insufficient or excessive filler content disrupts the matrix continuity or promotes filler agglomeration, which in turn leads to premature microcrack initiation and earlier failure. These findings align well with the tensile and SEM results, further confirming that moderate filler loading critically enhances both strength and ductility under complex loading modes such as bending. The gradual increase in stress with strain suggests efficient load transfer between the fiber, matrix, and filler, while the divergence in curves indicates variations in filler content or fiber alignment affecting mechanical properties. These results confirm the significant role of both banyan fibers and aluminium oxide in enhancing the composite's flexural strength.

### 3.3. *Izod impact strength*

Fig. 6 shows the impact strength of banyan fiber composite. Among

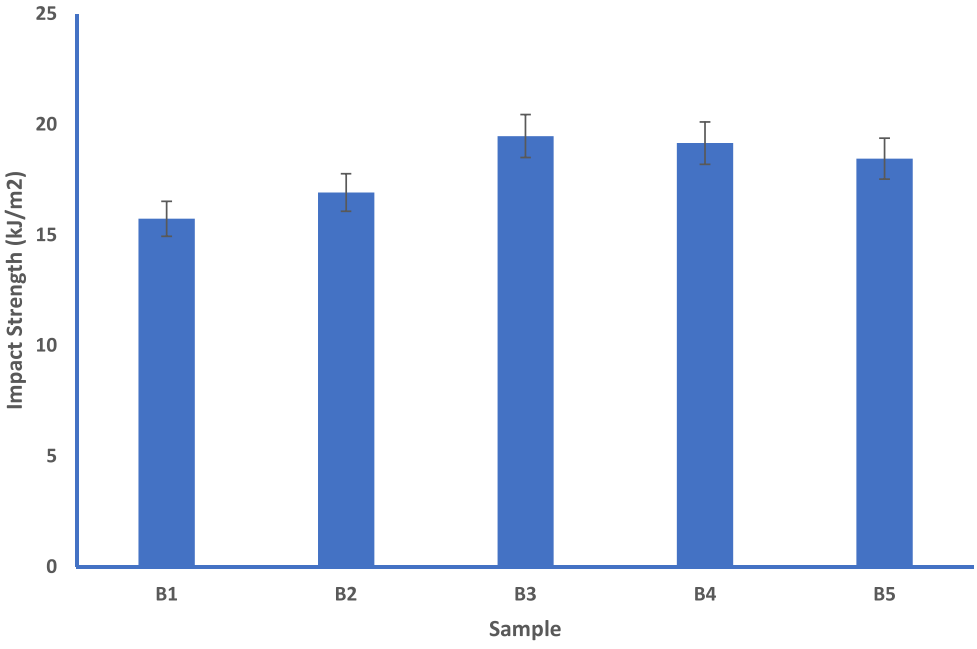


**Fig. 6.** Impact strength of banyan composite.

the five samples tested, Sample B3, which incorporated 3 % (12 g) $Al_2O_3$ filler, demonstrated the highest impact strength of 19.47 kJ/m$^2$. This result highlights the improved reinforcement achieved with this filler concentration, leading to efficient energy absorption and resistance to crack propagation during impact. In another work, the impact strength of pure epoxy is relatively low, 2.5 kJ/m$^2$, highlighting its susceptibility to fracture under dynamic loads [32]. The superior performance of B3 can be attributed to improved interfacial bonding between the fibers and matrix and the uniform dispersion of $Al_2O_3$ particles, which help in redistributing stress and enhancing toughness. In comparison, Sample B1, minimal filler content, exhibited the lowest impact strength of 15.73 kJ/m$^2$, reflecting its limited ability to resist impact due to weaker fiber-matrix interactions and the absence of reinforcing fillers. Sample B2, containing 2 % (8 g) $Al_2O_3$ filler, showed a slight improvement with an impact strength of 16.92 kJ/m$^2$, indicating a moderate enhancement in energy absorption capabilities due to partial reinforcement. Similarly, Sample B4 and Sample B5, with higher filler concentrations of 4 % (16 g) and 5 % (20 g), achieved impact strengths of 19.15 kJ/m$^2$ and 18.45 kJ/m$^2$, respectively. While these values are close to the maximum strength achieved by B3, they did not surpass it, likely due to filler particle agglomeration at higher concentrations, which can create localized stress points and reduce the composite's overall toughness. The results indicate that a 3 % (12 g) $Al_2O_3$ filler concentration provides a better balance between reinforcement and matrix integrity, resulting in the best energy dissipation characteristics. Similar research was found on the kenaf fiber-reinforced aluminium oxide particle epoxy matrix composites exhibit impressive impact strength enhancements, with values ranging from 8 kJ/m$^2$ to 15 kJ/m$^2$ for composites containing 15–25 % kenaf fibers and 1–5 % aluminium oxide particles. In comparison, banyan fiber-reinforced aluminium oxide particle epoxy composites typically achieve 15 kJ/m$^2$ to 19 kJ/m$^2$ under similar reinforcement conditions [33]. The superior impact strength of banyan fiber composites can be attributed to their higher toughness and better interfacial bonding with the matrix, which allows for more efficient energy dissipation during impact. While both composites offer excellent impact resistance, banyan fiber composites may be more suitable for applications requiring higher durability and resilience, such as heavy-duty protective structures. This finding suggests that Sample B3 is the most suitable composition for applications requiring materials with high impact resistance, such as in automotive crash components, protective gear, and structural panels in aerospace and construction.

### 3.4. Shore D hardness

Fig. 7 shows the shore D hardness of banyan fiber composite. Among the five samples tested, Sample B3, containing 3 % (12 g) $Al_2O_3$ filler, exhibited the highest Shore D hardness value of 47, indicating superior surface rigidity and reinforcement. This result demonstrates the effectiveness of the better filler content in enhancing the composite's hardness by improving the filler dispersion and interfacial adhesion between the fibers and the epoxy matrix, leading to a denser and more robust material structure. In another study, for pure epoxy matrix composite reveals the hardness, measured on the Shore D scale, usually falls with 28, demonstrating moderate surface resistance [34]. In comparison, Sample B1, minimal filler content, recorded the lowest Shore D hardness of 38, reflecting the absence of significant reinforcement and a less rigid surface. Sample B2, with 2 % (8 g) $Al_2O_3$ filler, showed an improvement in hardness, achieving a value of 41, which indicates the positive contribution of filler addition to the material's surface resistance. Similarly, Sample B4 and Sample B5, with 4 % (16 g) and 5 % (20 g) $Al_2O_3$ filler concentrations, demonstrated Shore D hardness values of 45 and 43, respectively. While these values are higher than those of B1 and B2, they fall slightly short of the maximum hardness achieved by B3. The marginal decrease in hardness at higher filler concentrations is likely due to particle agglomeration, which reduces the effective filler-matrix interaction and creates micro-defects, compromising surface uniformity and strength. The results indicate that a 3 % (12 g) $Al_2O_3$ filler concentration provides the significant balance for achieving maximum surface hardness without compromising the material's structural integrity. This enhanced hardness makes Sample B3 highly suitable for applications requiring materials with high surface durability and resistance to wear, such as in automotive panels, protective coverings, and industrial components. Uniform dispersion ensures that $Al_2O_3$ particles are evenly distributed throughout the matrix, preventing the formation of stress concentration points that could initiate cracks. The dispersed particles act as effective crack arrestors by interrupting crack propagation paths, redistributing the applied stress, and enhancing energy dissipation during loading. This mechanism contributes to the superior tensile strength of 67.49 MPa and improved impact energy of 19.47 kJ/m$^2$ observed in Sample B3. Additionally, the even dispersion improves fiber-matrix bonding, allowing for more efficient stress transfer, which further reinforces the composite's mechanical integrity. These enhancements collectively position Sample B3 as the improved

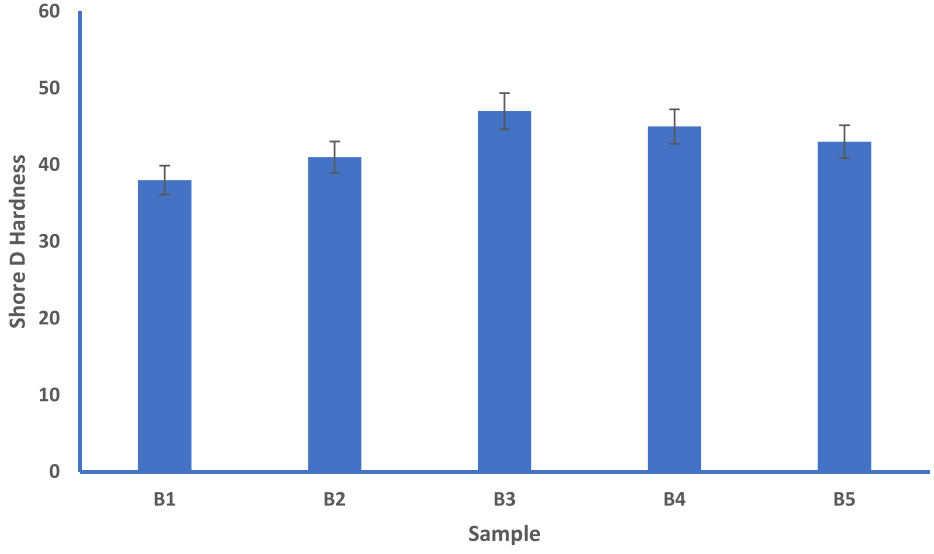


**Fig. 7.** Shore D hardness of banyan fiber composite.

configuration for balanced mechanical performance.

### 3.5. SEM & EDX analysis of banyan fiber composite

The SEM analysis of the tensile fractured surfaces of banyan fiber-reinforced $Al_2O_3$ particle filler blended epoxy matrix composites provides detailed insights into the interplay between fiber-matrix adhesion, filler dispersion, and the resulting mechanical behavior. The fractured surface of Sample B1 (1 % $Al_2O_3$ filler) highlights multiple defects, including significant fiber pull-outs and matrix cracks, which are clear indications of weak interfacial adhesion. These pull-outs suggest that the tensile stress was not adequately transferred from the matrix to the fibers, resulting in poor reinforcement efficiency. The presence of microvoids further indicates incomplete bonding or improper curing, which could have introduced stress concentration points, accelerating the initiation and propagation of cracks under tensile load [35]. These observations point to insufficient filler content in the matrix, which likely limited its ability to reinforce the composite and distribute stress effectively. In comparison, Sample B3 (3 % $Al_2O_3$ filler) demonstrates a more uniform dispersion of the $Al_2O_3$ particles within the epoxy matrix, which plays a pivotal role in enhancing the mechanical properties of the composite. The even distribution of the fillers ensures better load transfer between the matrix and the fibers, reducing the likelihood of stress concentrations and improving the tensile strength of the composite. The SEM image for this sample shows a significant reduction in fiber pull-outs and matrix cracking, indicating improved fiber-matrix bonding and enhanced energy dissipation during tensile deformation [36]. This uniform dispersion also suggests that the 3 % filler content strikes a balance between achieving sufficient reinforcement and avoiding the negative effects of filler agglomeration. The absence of large voids or significant fiber damage highlights the effectiveness of this formulation, making it the better filler concentration for achieving superior mechanical performance. On the other hand, Sample B5 (5 % $Al_2O_3$ filler) reveals a different fracture morphology, characterized by pronounced fiber cracking and noticeable agglomeration of $Al_2O_3$ particles. The SEM image shows clusters of filler particles, which act as stress concentrators, weakening the composite structure. These agglomerates not only compromise the load-bearing capacity of the composite but also hinder effective stress distribution, leading to localized failures [37]. Additionally, the excessive filler content in Sample B5 appears to disrupt the fiber-matrix interfacial bonding, reducing the composite's overall mechanical performance compared to Sample B3. The fiber cracks observed in this sample suggest that the excessive fillers may have caused internal stresses or brittleness within the matrix, further exacerbating the failure mechanisms. This highlights the detrimental impact of overloading the matrix with fillers, as it undermines the intended reinforcing effect and results in suboptimal material performance. The enhanced bonding and particle reinforcement contribute to the superior tensile strength of Sample B3 (67.49 MPa), as the composite is better equipped to withstand tensile forces without failure. The observed differences in failure mechanisms between Sample B5 and Sample B3 are further justified by the structural role of $Al_2O_3$ particles. In Sample B3, the ceramic fillers provide increased stiffness and enhance the matrix's ability to distribute stress uniformly, reducing the likelihood of localized stress concentration points, showing a void density of 2.3 % and shorter fiber pull-out lengths (12.4 μm) at 3 % $Al_2O_3$ filler, indicating strong bonding, compared to higher void density and pull-out lengths at 5 % filler due to weaker adhesion. Fig. 8 shows the SEM microstructure of banyan fiber composite. Elemental analysis of banyan fiber composite was given the Table 6.

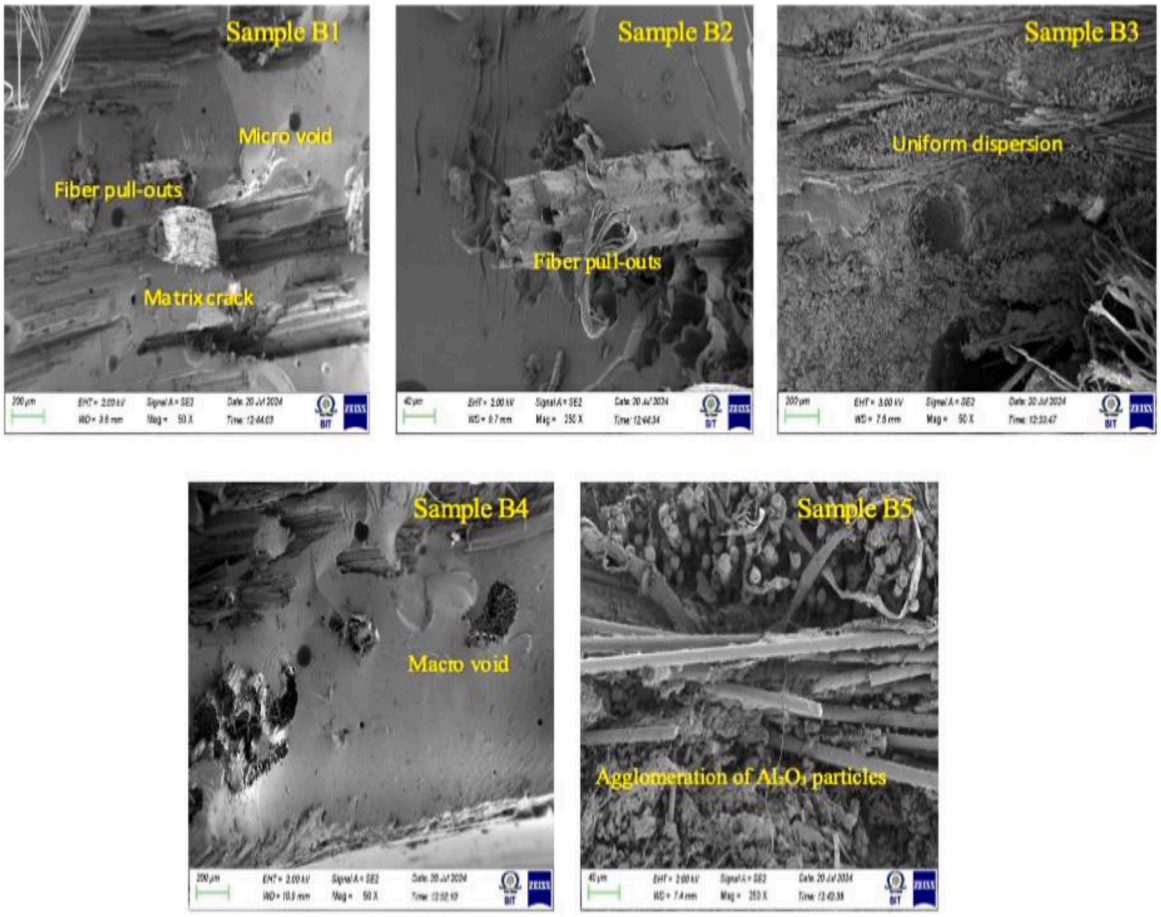


**Fig. 8.** The SEM microstructure of banyan fiber composite.

**Table 6**
Elements present in the banyan fiber composite.

| Element | Weight % | Atomic % | Error % | Net Int. | R | A | F |
|---|---|---|---|---|---|---|---|
| C K | 73.93 | 80.11 | 9.56 | 2616.90 | 0.9357 | 0.1815 | 1.0000 |
| O K | 24.17 | 19.66 | 11.34 | 748.29 | 0.9436 | 0.0662 | 1.0000 |
| Al L | 1.50 | 0.21 | 6.82 | 255.11 | 0.9640 | 0.8460 | 1.0025 |
| Na M | 0.03 | 0.00 | 63.90 | 3.27 | 0.9668 | 0.8964 | 1.0052 |
| Ca M | 0.37 | 0.02 | 22.70 | 43.17 | 0.9685 | 0.9183 | 1.0066 |

### *3.6. Fatigue behaviour of banyan fiber composite*

The fatigue behavior of banyan fiber composites was evaluated under cyclic loading to assess their durability and resistance to crack propagation. The results demonstrate that Sample B3, exhibits the most significant fatigue performance among the five tested samples. Sample B3 sustained an initial stress level of 40 MPa for up to 14,000 cycles, indicating superior resistance to fatigue-induced failure. This performance is attributed to the best concentration of $Al_2O_3$ particles, which are uniformly dispersed in the matrix, enhancing load distribution and acting as crack arrestors. The strong interfacial bonding between the fibers and the matrix in Sample B3 ensures efficient load transfer, minimizing stress concentration and delaying crack initiation and propagation. In contrast, Sample B1, with minimal filler, showed the poorest fatigue performance, failing at around 7000 cycles under similar stress levels. The rapid degradation in fatigue strength is due to weak fiber-matrix adhesion, poor load transfer, and the absence of reinforcement, which leaves the matrix vulnerable to crack formation and growth under repeated loading. In another research work, the hemp fiber-reinforced aluminium oxide particle epoxy matrix composites exhibit fatigue strength values ranging from 20 MPa to 45 MPa at $10^4$ cycles, with reinforcement levels of 20–30 % hemp fibers and 1 to 5 % aluminium oxide particles. In comparison, banyan fiber-reinforced aluminium oxide particle epoxy composites show slightly superior fatigue strength, ranging from 40 MPa to 50 MPa under similar reinforcement conditions [38]. The higher fatigue strength of banyan fiber composites can be attributed to their greater toughness and better bonding with the epoxy matrix, which enhances crack propagation resistance during cyclic loading. While both composites are suitable for lightweight structural applications under fatigue conditions, banyan fiber composites may be more advantageous for demanding applications requiring higher endurance and durability, such as in heavy-duty automotive and aerospace components. The lack of filler also means that the matrix is less able to absorb and redistribute cyclic stresses, leading to early failure. Sample B2, exhibited moderate improvement, sustaining 39 MPa for 10,000 cycles, demonstrating that the addition of filler enhances fatigue resistance by improving the composite's structural integrity. However, the lower filler concentration limits the reinforcement effect, resulting in suboptimal performance compared to B3. Similarly, Sample B4 and Sample B5, with higher filler concentrations of 4 % (16 g) and 5 % (20 g) respectively, performed better than B1 and B2, enduring 40 MPa for approximately 12,000 cycles and 10,000 cycles. Despite their improved performance, B4 and B5 showed slightly inferior results compared to B3, which can be justified by the potential agglomeration of $Al_2O_3$ particles at higher concentrations. This agglomeration leads to uneven stress distribution and creates localized stress concentration points, accelerating fatigue failure. Fig. 9 shows the fatigue behaviour of banyan fiber composite.

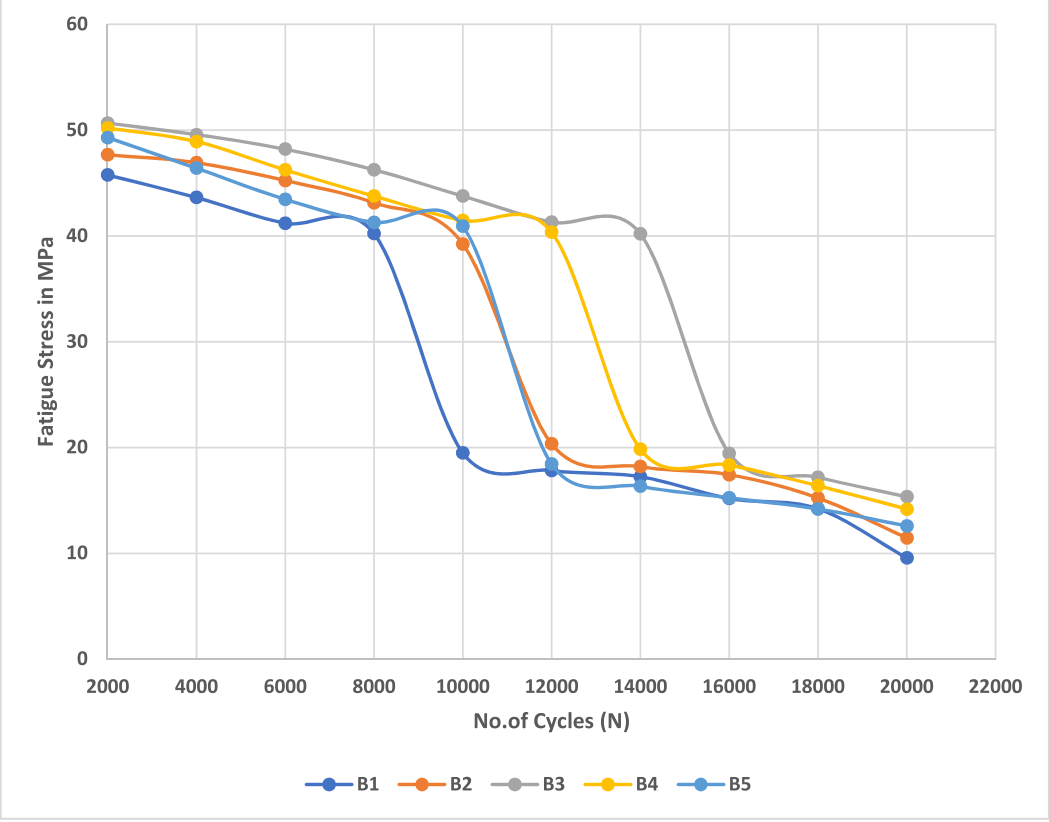


**Fig. 9.** The fatigue behaviour of banyan fiber composite.

The findings strongly justify the superior performance of Sample B3, the $Al_2O_3$ particles achieve good dispersion, reinforcing the matrix and improving its ability to resist crack propagation under cyclic loading. Additionally, the balance between particle reinforcement and fiber-matrix bonding ensures that stress is evenly distributed across the composite structure, reducing the likelihood of premature failure. The fatigue failure surfaces of B3, observed under SEM, further confirm the cohesive failure within the matrix, as opposed to interfacial debonding or fiber pull-out seen in B1, validating the improved bonding and integrity of B3. This enhanced fatigue behavior makes Sample B3 ideal for dynamic load-bearing applications in industries such as automotive, aerospace, and construction, where materials are exposed to repetitive loading and require high durability. The dispersed $Al_2O_3$ particles act as effective barriers to crack growth by interrupting the propagation path, redistributing stress, and increasing energy dissipation during cyclic loading. This mechanism significantly enhances the fatigue resistance of the composite, as demonstrated by Sample B3 sustaining 14,000 cycles at 40 MPa. In another research work, jute fiber-reinforced composites and flax-based epoxy composites exhibit fatigue lives of approximately 8000–10,000 cycles at comparable stress levels, primarily due to less effective crack mitigation strategies. The superior performance of the banyan fiber-reinforced composite with $Al_2O_3$ fillers highlights the advantages of uniform particle dispersion and strong fiber-matrix bonding in improving fatigue resistance. This performance is attributed to the uniform dispersion of $Al_2O_3$ particles within the matrix, which enhances stress distribution and minimizes localized stress concentrations during cyclic loading. The evenly distributed particles act as barriers to crack initiation and propagation, effectively delaying fatigue failure. Additionally, the strong fiber-matrix adhesion in Sample B3, achieved through best filler concentration and chemical treatment, enables efficient load transfer and energy dissipation, further enhancing fatigue resistance. These synergistic effects contribute to the exceptional durability of Sample B3 under repeated loading conditions. Therefore, the study underscores the importance of filler loading, as improper filler concentrations can lead to performance trade-offs, highlighting 3 % $Al_2O_3$ as the good content for achieving the best balance between fatigue strength and composite integrity.

### 3.7. Antibacterial activity of banyan fiber composite

The antibacterial activity of the banyan fiber composite Sample B3, was evaluated against *Streptococcus pyogenes* using the agar well diffusion method. The composite demonstrated significant antibacterial properties, as evidenced by the formation of a clear inhibition zone around the sample wells. When 100 μg of the composite was tested, it exhibited an inhibition zone of 12 mm, indicating a strong antibacterial effect. In comparison, a lower concentration of 50 μg produced an inhibition zone of 9 mm, showing a dose-dependent relationship between the composite concentration and its antibacterial efficacy. As a control, *Streptomycin* (10 μg), a standard antibiotic, exhibited a slightly higher inhibition zone of 15 mm, serving as a benchmark for evaluating the antibacterial potential of the composite. The antibacterial performance of Sample B3 can be attributed to the synergistic effects of the $Al_2O_3$ particles and the epoxy matrix. The $Al_2O_3$ particles are known for their intrinsic antimicrobial properties, which disrupt bacterial cell membranes and inhibit growth. Their uniform dispersion within the composite ensures consistent antibacterial action across the material surface. Additionally, the high surface area of the $Al_2O_3$ nanoparticles increases contact with bacterial cells, enhancing their efficacy. The banyan fiber-epoxy matrix provides a stable framework, allowing prolonged antimicrobial action and ensuring that the material retains its functionality over time. The results confirm that the inclusion of 3 % $Al_2O_3$ not only enhances the mechanical and thermal properties of the composite but also imparts significant antibacterial activity, making it suitable for applications in environments prone to bacterial contamination. This includes potential use in biomedical applications (e.g., wound dressings or hospital equipment), water filtration systems, and structural components in humid or bioactive environments. Chemically, $Al_2O_3$ generates reactive oxygen species (ROS) on its surface, which induce oxidative stress in bacterial cells, damaging their membranes, proteins, and DNA, ultimately leading to cell death. This oxidative mechanism is particularly effective against Gram-positive bacteria like Streptococcus pyogenes, as observed in this study. Physically, $Al_2O_3$ nanoparticles exhibit high hardness and sharp edges, which disrupt bacterial cell walls upon contact, causing membrane rupture and leakage of intracellular contents. These dual mechanisms work synergistically, enhancing the antibacterial efficacy of the composite [39]. It was noted that higher concentrations of $Al_2O_3$ showed larger inhibition zones, indicating a strong correlation between dosage and antibacterial efficacy. This dose-dependent behavior could be tailored for specific applications by adjusting the filler concentration to meet the antibacterial requirements of different environments. For instance, higher doses could be used in critical biomedical applications, such as coatings for hospital equipment, where strong antibacterial properties are essential, while moderate doses could suffice for hygienic construction materials. The dose-dependent behavior observed further highlights the flexibility of tailoring antibacterial efficacy by varying filler concentrations, making Sample B3 a versatile material for multifunctional applications. These findings establish banyan fiber composite Sample B3 as a potential material for antibacterial applications while maintaining its mechanical integrity. Fig. 10 shows the antibacterial activity of banyan fiber composite.

### 3.8. Biofilm analysis of banyan fiber composite

The biofilm analysis of banyan fiber composite Sample B3, was conducted using CLSM with dual staining via Acridine Orange (AO) and Propidium Iodide (PI) to visualize live and dead bacterial cells and evaluate its anti-biofilm efficacy against *Streptococcus pyogenes*. The control group (a, b, c) and the composite sample (d, e, f) were compared to highlight the impact of the composite's antibacterial properties on biofilm formation and bacterial viability. In the control group (a, b, c), the CLSM images stained with Acridine Orange (green fluorescence) demonstrate dense bacterial colonization and intact biofilm formation, indicating the proliferation of live bacterial cells without disruption [40]. The absence of Propidium Iodide fluorescence (red, indicative of dead cells) further confirms that bacterial cells in the control sample were predominantly viable, allowing for robust biofilm development. The overlaid image (c) illustrates a uniform green signal, highlighting the structural integrity and resilience of the biofilm in the absence of antibacterial interference. Fig. 11 shows the biofilm analysis of banyan fiber composite.

In contrast, the CLSM analysis of Sample B3 (d, e, f) shows significant disruption in the biofilm structure, indicating a strong antibacterial effect. Acridine Orange staining (d) reveals a marked reduction in the population of live bacterial cells compared to the control. Simultaneously, the Propidium Iodide staining (e) exhibits intense red fluorescence, signalling widespread bacterial cell death. The overlaid image (f) presents a combination of live (green) and dead (red) bacterial populations, with a predominant red signal in regions of disrupted biofilm. This dual staining pattern clearly demonstrates that Sample B3 effectively inhibits biofilm formation and induces bacterial cell death, disrupting the biofilm's viability and structural integrity. The antibacterial activity of Sample B3 is primarily attributed to the inclusion of $Al_2O_3$ particles, which exhibit intrinsic antimicrobial properties. These particles disrupt bacterial cell walls and membranes through physical and chemical interactions, such as oxidative stress and nanoparticle-induced mechanical disruption [41]. The uniform dispersion of $Al_2O_3$ particles within the composite ensures consistent antibacterial activity across the surface, reducing bacterial adhesion and biofilm establishment. Furthermore, the strong interfacial bonding between the banyan fibers and the $Al_2O_3$-reinforced epoxy matrix provides a stable platform for

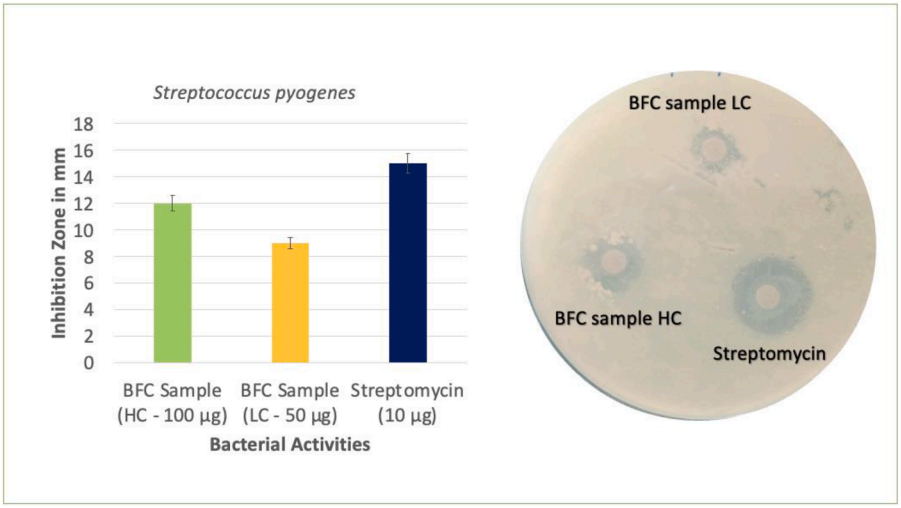


**Fig. 10.** The antibacterial activity of banyan fiber composite.

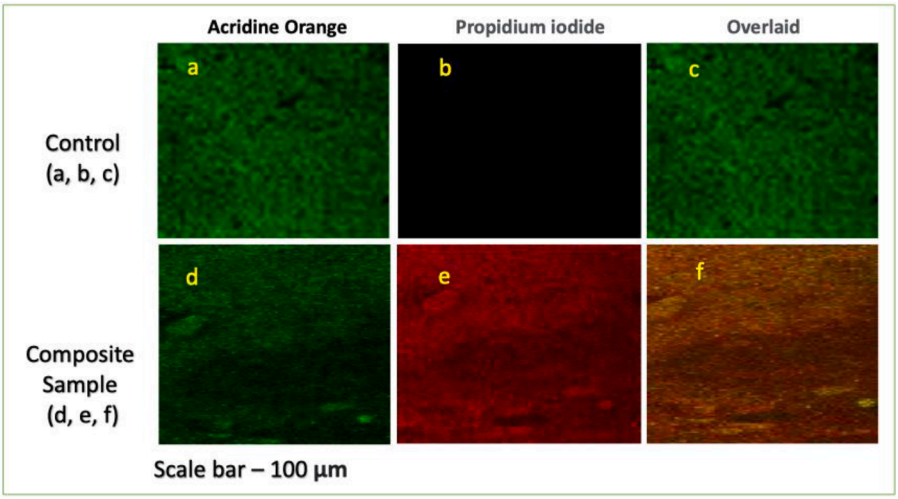


**Fig. 11.** The biofilm analysis of banyan fiber composite.

sustained antibacterial action. The results justify the enhanced anti-biofilm efficacy of Sample B3. The visible reduction in live bacteria and biofilm disruption confirm the composite's ability to combat *Streptococcus pyogenes*, a biofilm-forming pathogen associated with persistent infections. The biomedical implications of biofilm disruption were emphasized. The observed ability of the composite to significantly reduce live bacterial populations and prevent biofilm formation suggests its potential as a bioactive material for environments prone to bacterial contamination. Applications could include use in surgical instruments, implantable devices, or antimicrobial surfaces in healthcare facilities, as well as hygienic materials in public spaces. This makes Sample B3 highly suitable for applications requiring antimicrobial and anti-biofilm materials, such as medical devices, wound dressings, water filtration systems, and structural materials in hygienic environments.

## 4. Limitations of this research work

While the developed composite exhibits encouraging mechanical and antibacterial properties, several limitations was acknowledged to guide future research. Firstly, the study did not include comprehensive biocompatibility assessments such as cytotoxicity tests or in vivo evaluations, which are essential for confirming its safety and efficacy in medical applications. Additionally, the long-term stability of the composite under physiological and environmental stressors such as moisture absorption, thermal cycling, and UV exposure was not investigated, which may influence its structural integrity and functional lifespan. Although antibacterial efficacy was demonstrated, the underlying mechanisms whether attributed to $Al_2O_3$ nanoparticle activity, fiber surface characteristics, or their synergistic effect were not systematically analyzed. Moreover, the composite's resistance to conventional sterilization processes (e.g., autoclaving, gamma irradiation) remains untested, posing a barrier to immediate clinical translation. The mechanical characterization was also limited in scope, with fatigue performance assessed under a single load condition and no evaluation of other critical behaviours such as creep, wear resistance, or impact fatigue. Finally, the hand layup method employed, while effective for laboratory-scale fabrication, may pose scalability challenges in terms of process control and uniformity in industrial settings. Addressing these limitations will be vital for advancing the material toward practical use in biomedical and structural applications.

## 5. Conclusion

This study successfully developed and characterized an epoxy matrix composite reinforced with $Al_2O_3$-embedded banyan fibers, demonstrating significant improvements in mechanical performance, fatigue

resistance, and antibacterial functionality. Among the tested formulations, Sample B3 exhibited optimal performance, with a tensile strength of 67.49 MPa (an 8.9 % increase), flexural strength of 69.38 MPa (7.2 % increase), and impact energy of 19.47 kJ/m$^2$ (21 % increase) compared to the control. Shore D hardness also improved by 19 %, reflecting enhanced surface durability due to the homogeneous dispersion of $Al_2O_3$ nanoparticles. Fatigue analysis confirmed the composite's ability to sustain cyclic stress (40 MPa) over 14,000 cycles, representing a 14.8 % increase in fatigue life. SEM imaging corroborated these findings, revealing improved interfacial adhesion, reduced voids, and consistent filler distribution. Antibacterial testing against Streptococcus pyogenes showed a 12 mm inhibition zone, while Confocal Laser Scanning Microscopy demonstrated substantial biofilm disruption and a marked reduction in viable bacterial populations, attributable to the antimicrobial activity of the embedded $Al_2O_3$ nanoparticles. These multifunctional characteristics position the developed composite as a potential material for secondary structural applications in sectors such as automotive and aerospace, where a balance of mechanical strength and fatigue resistance is critical. Furthermore, the demonstrated antibacterial and anti-biofilm properties suggest potential utility in the healthcare sector, particularly for use in non-load-bearing medical components such as orthopaedic supports, antimicrobial panels, prosthetic shells, and hygienic surfaces in clinical environments. However, immediate clinical implementation is not yet feasible. Further research is required to assess biocompatibility, sterilization resistance, and long-term performance under physiological conditions. Additionally, scaling the fabrication process from laboratory to industrial production will be essential to ensure consistency, reproducibility, and regulatory compliance. Therefore, while the developed composite exhibits significant potential, targeted follow-up studies are necessary to fully enable its adoption in industrial and biomedical applications.

## Future scope of the research work

The future research exploring hybrid fillers, combining $Al_2O_3$ with other nanoparticles such as $SiO_2$ or $TiO_2$, to achieve synergistic effects that could further improve mechanical strength, thermal stability, and antibacterial efficacy. Additionally, advanced fabrication techniques, such as resin transfer molding or additive manufacturing, are proposed to enhance filler dispersion, reduce void content, and improve the scalability of the composites. These directions aim to build upon the current study's findings and drive further advancements in the development of high-performance, multifunctional composites.

## CRediT authorship contribution statement

**Baskar S:** Investigation, Funding acquisition, Formal analysis. **Ganesan Subbiah:** Supervision, Software, Resources. **Padma Priya G:** Software, Resources. **Guntaj J:** Supervision, Software, Resources. **Mukesh Kumar:** Resources, Project administration, Methodology. **Kamakshi Priya K:** Resources, Funding acquisition. **Nandagopal Kaliappan:** Formal analysis, Data curation, Conceptualization.

## Declaration of competing interest

The authors declare that they have no known competing financial interests or personal relationships that could have appeared to influence the work reported in this paper.

## Data availability

No data was used for the research described in the article.

## References


[1] A. Jamaldar, P. Asadi, M. Salimi, M. Payan, P.Z. Ranjbar, M. Arabani, H. Ahmadi, Application of natural and synthetic fibers in bio-based earthen composites: a state-of-the-art review, Result. Eng. (2024) 103732.

[2] B.K. Dejene, Exploring the potential of ZnO nanoparticle-treated fibers in advancing natural fiber reinforced composites: a review, J. Nat. Fiber. 21 (1) (2024) 2311304.

[3] T. Raja, Innovative lightweight materials using sugarcane ash and neem fiber epoxy matrix composite for sustainable applications, Result. Eng. (2024) 103720.

[4] A. Akhyar, M. Ibrahim, M. Rizal, A. Riza, A. Farhan, M. Bahi, U. Muzakir, The effect of differences in fiber sizes on the cutting force during the drilling process of natural fiber-reinforced polymer composites, Result. Eng. 24 (2024) 103128.

[5] T. Raja, Y. Devarajan, P. Jayasankar, D. Singh, G. Subbiah, K. Logesh, Characterization and Sustainable Applications of Galinsoga parviflora Natural Fibers: a Pathway to Eco-Friendly Material Development, Result. Eng. (2024) 103601.

[6] G. Ravindran, V. Mahesh, N. Bheel, S. Chittimalla, K. Srihitha, A. Sushmasree, Usage of natural fibre composites for sustainable material development: global research productivity analysis, Buildings 13 (5) (2023) 1260.

[7] D. Thapliyal, S. Verma, P. Sen, R. Kumar, A. Thakur, A.K. Tiwari, R.K. Arya, Natural fibers composites: origin, importance, consumption pattern, and challenges, J. Compos. Sci. 7 (12) (2023) 506.

[8] B.K. Dejene, Advancing natural fiber-reinforced composites through incorporating ZnO nanofillers in the polymeric matrix: a review, J. Nat. Fiber. 21 (1) (2024) 2356015.

[9] B.K. Dejene, A.D. Gudayu, M.A. Abtew, Development and optimization of sustainable and functional food packaging using false banana (Enset) fiber and zinc-oxide (ZnO) nanoparticle-reinforced polylactic acid (PLA) biocomposites: a case of Injera preservation, Int. J. Biol. Macromol. 279 (2024) 135092.

[10] M.H. Nazir, A.H. Al-Marzouqi, W. Ahmed, E. Zaneldin, The potential of adopting natural fibers reinforcements for fused deposition modeling: characterization and implications, Heliyon 9 (4) (2023).

[11] T. Raja, Y. Devarajan, J.U. Prakash, V.J. Upadhye, L. Singh, S. Kannan, Sustainable innovations: mechanical and thermal stability in palm fiber-reinforced boron carbide epoxy composites, Result. Eng. 24 (2024) 103214.

[12] N.K. Gupta, S.K. Joshi, S. Dhama, S. Aggarwal, Enhancing mechanical properties of natural fiber composites: a study on the effects of fiber loading and filler addition, Eng. Res. Express 5 (4) (2023) 045088.

[13] A. Soni, S. Kumar, B. Majumder, H. Dam, V. Dutta, P.K. Das, Synergy of waste plastics and natural fibers as sustainable composites for structural applications concerning circular economy, Environ. Sci. Pollut. Res. 31 (27) (2024) 38846–38865.

[14] M.K. Marichelvam, C.L. Kumar, K. Kandakodeeswaran, B. Thangagiri, K.K. Saxena, K. Kishore, S. Kumar, Investigation on mechanical properties of novel natural fiber-epoxy resin hybrid composites for engineering structural applications, Case Stud. Construct. Mater. 19 (2023) e02356.

[15] J.S. Ahmed, K. Satyasree, R.R. Kumar, O. Meenakshisundaram, S. Shanmugavel, A comprehensive review on recent developments of natural fiber composites synthesis, processing, properties, and characterization, Eng. Res. Express 5 (3) (2023) 032001.

[16] M. Pokhriyal, P.K. Rakesh, S.M. Rangappa, S. Siengchin, Effect of alkali treatment on novel natural fiber extracted from Himalayacalamus falconeri culms for polymer composite applications, Biomass Convers. Biorefin. 14 (16) (2024) 18481–18497.

[17] B. Szadkowski, A. Marzec, M. Kuśmierek, M. Piotrowska, D. Moszyński, Functionalization of bamboo fibers with lawsone dye (Lawsonia inermis) to produce bioinspired hybrid color composite with antibacterial activity, Int. J. Biol. Macromol. 259 (2024) 129178.

[18] D. Liu, A.M. Pourrahimi, R.T. Olsson, M.S. Hedenqvist, U.W. Gedde, Influence of nanoparticle surface treatment on particle dispersion and interfacial adhesion in low-density polyethylene/aluminium oxide nanocomposites, Eur. Polym. J. 66 (2015) 67–77.

[19] K.R. Sumesh, K. Kanthavel, Green synthesis of aluminium oxide nanoparticles and its applications in mechanical and thermal stability of hybrid natural composites, J. Polym. Environ. 27 (2019) 2189–2200.

[20] S. Bhavsar, G.B. Patel, N.L. Singh, Investigation of optical properties of aluminium oxide doped polystyrene polymer nanocomposite films, Phys. B: Condens. Matter. 533 (2018) 12–16.

[21] M.M. Rahman, M. Maniruzzaman, M.S. Yeasmin, A state-of-the-art review focusing on the significant techniques for naturally available fibers as reinforcement in sustainable bio-composites: extraction, processing, purification, modification, as well as characterization study, Result. Eng. 20 (2023) 101511.

[22] S.M. Hasan, R.S. Thompson, H. Emery, A.L. Nathan, A.C. Weems, D.J. Maitland, Modification of shape memory polymer foams using tungsten, aluminum oxide, and silicon dioxide nanoparticles, RSC Adv. 6 (2) (2016) 918–927.

[23] L. Zamora-Mendoza, E. Guamba, K. Miño, M.P. Romero, A. Levoyer, J.F. Alvarez-Barreto, F. Alexis, Antimicrobial properties of plant fibers, Molecules 27 (22) (2022) 7999.

[24] S. Jayabal, S. Sathiyamurthy, K.T. Loganathan, S. Kalyanasundaram, Effect of soaking time and concentration of NaOH solution on mechanical properties of coir–polyester composites, Bull. Mater. Sci. 35 (4) (2012) 567–574.

[25] T. Kanthiya, P. Rachtanapun, S. Boonrasri, T. Kittikorn, T. Chaiyaso, P. Worajittiphon, K. Jantanasakulwong, Reinforcement of Epoxidized Natural Rubber with High Antimicrobial Resistance Using Water Hyacinth Fibers and Chlorhexidine Gluconate, Polymers (Basel) 16 (21) (2024) 3089.

[26] T.R. Indumathi, R. Divya, B.S. Kumar, A. Selvakumar, Antimicrobial study on surface-coated Hibiscus sabdariffa L. fiber reinforcement, Biomass Convers. Biorefin. 14 (20) (2024) 25239–25250.
[27] R. Yadav, A. Meena, Effect of aluminium oxide, titanium oxide, hydroxyapatite filled dental restorative composite materials on physico-mechanical properties, Ceram. Int. 48 (14) (2022) 20306–20314.
[28] S. Vellaiyan, D. Chandran, R. Venkatachalam, K. Ramalingam, R. Rao, R. Raviadaran, Maximizing waste plastic oil yield and enhancing energy and environmental metrics through pyrolysis process optimization and fuel modification, Res. Eng. 22 (2024) 102066.
[29] S.A. Prasath, V. Balamurugan, S.S. Ganesh, A.U. Murthy, Evaluation of mechanical properties on banyan fiber reinforced polymer matrix composite using FEA, in: IOP Conference Series: Materials Science and Engineering, August 402, IOP Publishing, 2018 012135.
[30] R. Kochetov, A.V. Korobko, T. Andritsch, P.H.F. Morshuis, S.J. Picken, J.J. Smit, Modelling of the thermal conductivity in polymer nanocomposites and the impact of the interface between filler and matrix, J. Phys. D Appl. Phys. 44 (39) (2011) 395401.
[31] R. Thandavamoorthy, Y. Devarajan, N. Kaliappan, Antimicrobial, function, and crystalline analysis on the cellulose fibre extracted from the banana tree trunks, Sci. Rep. 13 (1) (2023) 15301.
[32] B. Zuccarello, C. Militello, F. Bongiorno, Fatigue behaviour of high-performance green epoxy biocomposite laminates reinforced by optimized long sisal fibers, Polym. (Basel) 16 (18) (2024) 2630.
[33] M. Nadeem, N.H.H. Betrico, R.P. Devarajalu, V. Gopalan, V. Prakasam, M. R. Degalahal, S.V. Pitchumani, Virtual fatigue life prediction of cellulose microfibrils reinforced polymer composite, Brazil. Arch. Biol. Technol. 67 (2024) e24240029.
[34] K. Venkatesan, S. Rajaram, I. Jenish, G.B. Bhaskar, Fatigue and creep behavior of abaca–sisal natural fiber–reinforced polymeric composites, Biomass Convers. Biorefin. 14 (16) (2024) 19961–19972.
[35] A. Fotouh, J.D. Wolodko, M.G. Lipsett, Fatigue of natural fiber thermoplastic composites, Compos. Part B: Eng. 62 (2014) 175–182.
[36] S. Bhowmik, S. Kumar, V.K. Mahakur, Various factors affecting the fatigue performance of natural fiber-reinforced polymer composites: a systematic review, Iran. Polym. J. 33 (2) (2024) 249–271.
[37] H. Savastano Jr, S.F.D. Santos, M. Radonjic, W.O Soboyejo, Fracture and fatigue of natural fiber-reinforced cementitious composites, Cement Concret. Compos. 31 (4) (2009) 232–243.
[38] R. Thandavamoorthy, Y. Devarajan, S. Thanappan, Analysis of the characterization of NaOH-treated natural cellulose fibre extracted from banyan aerial roots, Sci. Rep. 13 (1) (2023) 12579.
[39] B.P. Rocky, A.J. Thompson, Production of natural bamboo fiber - 2: assessment and comparison of antibacterial activity, AATCC J. Res. 6 (5) (2019) 1–9.
[40] A. Vinod, M.R. Sanjay, S. Suchart, P. Jyotishkumar, Renewable and sustainable biobased materials: an assessment on biofibers, biofilms, biopolymers and biocomposites, J. Clean. Prod. 258 (2020) 120978.
[41] O.B. Gutiérrez-Acosta, S. Arriaga, V.A. Escobar-Barrios, S. Casas-Flores, A. Almendarez-Camarillo, Performance of innovative PU-foam and natural fiber-based composites for the biofiltration of a mixture of volatile organic compounds by a fungal biofilm, J. Hazard. Mater. 201 (2012) 202–208.